INTERNATIONAL JOURNAL OF ROBUST AND NONLINEAR CONTROL
Int. J. Robust Nonlinear Control 2016; **26**:1267–1285
Published online 8 January 2016 in Wiley Online Library (wileyonlinelibrary.com). DOI: 10.1002/rnc.3502

Adaptive perimeter traffic control of urban road networks based on MFD model with time delays

Jack Haddad*,† and Boris Mirkin

Technion Sustainable Mobility and Robust Transportation (T-SMART) Laboratory, Faculty of Civil and Environmental Engineering, Technion – Israel Institute of Technology, Haifa, Israel

SUMMARY

In this work, we focus on two main themes: (i) developing a more realistic macroscopic fundamental diagram-based nonlinear control-oriented model of urban traffic networks with time delays incorporated into model structure; and (ii) based on its linearized form subject to input delay, designing two new perimeter control architectures for one aggregated urban traffic region under unknown bounded external disturbances and parameter uncertainties. The feedback control laws design is performed in the context of model reference adaptive control approach. Simulation results based on a linearized model are also presented, which demonstrate in this case desired closed-loop adaptive control system performance. Copyright © 2016 John Wiley & Sons, Ltd.

Received 9 December 2014; Revised 6 September 2015; Accepted 16 November 2015

KEY WORDS: macroscopic fundamental diagram (MFD); feedback traffic control; adaptation; input delays

1. INTRODUCTION

Perimeter feedback control, based on macroscopic fundamental diagram (MFD) concept, is one of the most promising and rapidly developing paradigms for controlling large-scale urban road networks. The main idea of perimeter feedback control is to manipulate the transfer flows at the perimeter borders of an urban region, in order to stabilize the number of vehicles in that region at a desired level; see, for example, [1–3] for single-region cities and [4–8] for multi-region cities.

Main trends of research activity in the framework of *the perimeter feedback control paradigm* can be classified into the following categories: (i) the design is based on nonlinear models – the model predictive control method [5, 7, 8]; and (ii) the design is based on linearized models – the classical PI feedback control for a single urban region [2]. Optimal linear-quadratic state feedback control (LQR) design for a multi-input multi-output problem [6], where two LQR versions of an optimization problem, without and with integral action, is studied; combination of switching signal timing plans and perimeter controllers for a large-scale urban network is proposed in [7, 9].

Point out that all the aforementioned papers deal only with (i) deterministic models, that is, without any parametric uncertainty and (ii) without taking into account the travel times needed for vehicles to reach the regional border, that is, dead time. At the same time, the inclusion of these important components in the models for feedback control strategies design is becoming a recognized trend in traffic feedback control [2, 3, 6, 10]. Indeed, uncertainties in MFDs and time delays are both vital ingredients to improve the modeling of real systems, whereas their presence requires the development of new design methods and realistic control schemes.

*Correspondence to: Jack Haddad, Technion Sustainable Mobility and Robust Transportation (T-SMART) Laboratory, Faculty of Civil and Environmental Engineering, Technion – Israel Institute of Technology, Haifa, Israel.
†E-mail: jh@technion.ac.il

As far as the authors know, [3] is the first study that takes into consideration model parameter uncertainties in the design of perimeter traffic feedback control. In [3], a robust fixed structure perimeter controller was designed for an urban region with the MFD representation including MFD uncertainty, which includes scatter of flows for the same accumulation. The MFD uncertainty has been realized in the model as parameter uncertainties.

While most of the previous MFD-based dynamic models utilized for design, for example, [3, 5, 7, 8], postulate that vehicles can *immediately* travel from the urban region to its border, in recent appeared papers [2, 6, 10], travel times were incorporated as a time delay in the control input of the MFD-based models for control law synthesis. In [2], for the gating control problem at an urban region, the time delay corresponding to the travel time needed for gated vehicles to approach the network is presented, while in [6], the control input delays are presented in the traffic flow dynamics for the perimeter control problem at multi-region systems. Note that the controller in [6] is designed assuming time delays equal to zero. While in [2, 10] the design is carried out in discrete time, and as it is well known, for example, [11], in this case, the presence of delay makes no principal difficulties in the synthesis, because it can be removed by expanding the state space of the plant model. In both cases, the parameters of the system model *are known*.

In this paper, our first goal is to introduce a new MFD-based model of urban traffic networks. The main contributions here by contrast to the results presented earlier, for example, in [5, 7], are as follows: (i) developing a more realistic nonlinear control-oriented dynamic traffic model built on the MFD concept by *incorporating into model structure the time-delay effects in the command transfer channels as a key critical (natural integral) factor in the context of perimeter control.* It is important to note that delays depend on the number of vehicles in region; that is, the time delays are state dependent. (ii) An additional novel element of the present paper is *the procedure* allowing to formalize representation of traffic dynamics in an interconnected state-space vector matrix form, relying on the fact that each region can communicate with the set of the other regions, whose number in general varies and changes the dimension of the state vector.

Based on the developed model, our second goal is to design two new adaptive control schemes that can lead to tractable design formulations for (i) state feedback, when the plant state is measured, that is, the number of vehicles from all regional origins to regional destinations are measured, and (ii) output feedback, when the system output is only measured, that is, only the total number of vehicles in all regions are measured.

2. MACROSCOPIC FUNDAMENTAL DIAGRAM (MFD) CONCEPT

Macroscopic fundamental diagrams provide aggregate relationships between traffic variables at urban networks; that is, the MFD can respectively link between network vehicle density (veh/km) or accumulation (veh) and network space-mean flow or trip completion flow (veh/hr). The MFD has the following link form: network flow increases as accumulation increases up to a critical accumulation where the flow is maximized, and if the accumulation increases beyond the critical one, then the flow decreases until it reaches zero at gridlock. The flows in networks are subjected to variations due to demand changes and various kinds of perturbation. To reflect such uncertainties for robust modeling, the MFD pattern is given by an admissible set of traffic data, with a scatter that becomes higher as accumulation increases [12–15]. That is, the relevant function that approximates the aggregate relationship between traffic variables is *an interval function* that might change within specified bounds. Such interval representation of the MFD shape is particularly important if MFD-based model is used for feedback traffic control design [3]. Figure 1 provides a shape of such partially uncertain (interval) MFD, where the blue curve corresponds the nominal MFD.

Modeling of transportation networks based on MFDs was initially proposed by [16], although their theoretical foundations (e.g., the existence of MFDs) were provided later by [1]. The MFDs were found to well describe the dynamics of a congested urban network first in Yokohama by [17] and were investigated using empirical or simulated data by [12, 13, 18–23] and others. Homogeneous (i.e., small variance of link densities) large networks have a well-defined MFD form (as observed in Yokohama), that is, low scatter of flows for the same densities (or accumulations), [12, 19, 24–26].

DOI: 10.1002/rnc

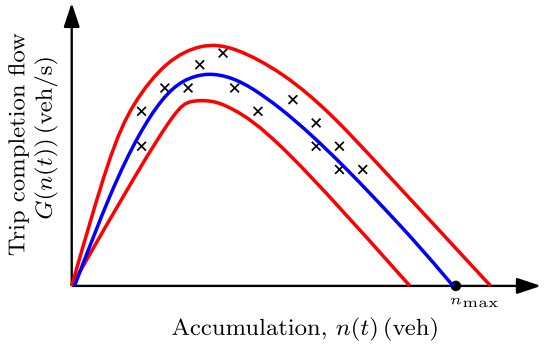

Figure 1. Typical interval shape of a macroscopic fundamental diagram.

Different MFD-based state-space dynamic models for control design, describing the traffic flow dynamics of separate or multi-region systems, have been found (in one form or another) relying on *vehicle conservation equations*. Mainly, such state-space dynamic models of each separate or interacting with other urban regions $R_i,\ i = 1, \ldots, R$, in, for example, works [1, 6], were formed based only on the integral regional accumulation $n_i(t)$(veh), and this variable is used as a *scalar* state variable of the dynamic models. To derive a more complete traffic flow dynamic, it was first suggested in [5] to take into account that the integral regional accumulation $n_i(t) \in \mathbb{R}$ includes both vehicles with destination to inside the region and vehicles with destination to outside the region. That is, the integral accumulation of each region $n_i(t)$ is split into some autonomous components $n_{ii}(t)$, defined as the number of vehicles from region i with destination to inside the region, and $n_{ij}(t)$ defined as the number of vehicles from region i with destination to regions $j,\ j \in S_i$. The variable S_i stands for the set of the regions, with which the region i can communicate, that is, the set of regions that are directly reachable from region i. Each of S_i is a set of integers corresponding to the region's index number. It was suggested in [5, 7] to use the integral regional accumulation $n_i(t)$ in the following decomposed form:

$$R_i : n_i(t) = n_{ii}(t) + \sum_{j \in S_i} n_{ij}(t)\,. \tag{1}$$

Therefore, in contrast to [1, 6], the separate region state in, for example, [5, 7], is a vector. For example, this vector has the form $[n_{11}(t),\ n_{12}(t)]^T \in \mathbb{R}^2$ (not $n_1(t) \in \mathbb{R} = n_{11}(t) + n_{12}(t)$) for the case of the single region control, and the form $[n_{11}(t),\ n_{12}(t),\ n_{22}(t),\ n_{21}(t)]^T \in \mathbb{R}^4$ with two interconnected regions.

3. CONTROL-ORIENTED MODEL DESIGN

3.1. Notations

We denote the MFD by $G_i(n_i(t))$ (veh/s), which is defined as the trip completion flow for region i at $n_i(t)$. The transfer flow from i with destination to j, denoted by $M_{ij}(n_{ii}(t), n_i(t))$ (veh/s), is calculated corresponding to the ratio between accumulations, that is, $M_{ij}(n_{ij}(t), n_i(t)) = n_{ij}(t)/n_i(t) \cdot G_i(n_i(t))$, and the internal flow from i with destination to i is calculated by $M_{ii}(n_{ii}(t), n_i(t)) = n_{ii}(t)/n_i(t) \cdot G_i(n_i(t))$. It is also assumed that $q_{ij}(t)$ (veh/s) is the traffic flow demand generated in region i with direct destination to region j. Furthermore, we introduce the following 'vectorization' symbols:

$$\begin{aligned} \mathbf{Vec}_{j=1}^{m} z_j &= [z_1, \cdots, z_m]^{\mathrm{T}}, \quad \mathbf{Dg}_{j=1}^{m} z_j = diag\{z_1, \cdots, z_m\}, \\ \mathbf{Mat}_{j=1}^{m} \frac{\partial z_j}{\partial v} &= \begin{bmatrix} \frac{\partial z_1}{\partial v_1} & \cdots & \frac{\partial z_1}{\partial v_p} \\ \vdots & \ddots & \vdots \\ \frac{\partial z_m}{\partial v_1} & \cdots & \frac{\partial z_m}{\partial v_p} \end{bmatrix}, \quad v = \begin{bmatrix} v_1 \\ \vdots \\ v_p \end{bmatrix}. \end{aligned} \tag{2}$$

The symbol $\mathrm{card}(S_i)$ denotes the cardinality (size) of S_i.

DOI: 10.1002/rnc

3.2. Revisited vehicle conservation model

To develop a realistic control-oriented mathematical model that incorporates time delay in its structure, first we write, based on [5, 7], the vehicle conservation equations of the R-region MFDs system

$$\begin{aligned}
\dot{n}_{ii}(t) &= -M_{ii}(n_{ii}(t), n_i(t)) + \sum_{j \in S_i} M_{ji}(n_{ji}(t), n_j(t)) u_{ji}(t) + q_{ii}(t), \\
\dot{n}_{ij}(t) &= -M_{ij}(n_{ij}(t), n_i(t)) u_{ij}(t) + q_{ij}(t), \\
n_i(t) &= n_{ii}(t) + \sum_{j \in S_i} n_{ij}(t), \\
u_{ij}(t) + u_{ji}(t) &= \epsilon_{ij},
\end{aligned} \tag{3}$$

where $u_{ij}(t)$ and $u_{ji}(t)$ $(-)$, $i = 1, 2, \ldots, R$ and $j \in S_i$, denote the perimeter control inputs, which are introduced on the border between the regions i and j, to control the transfer flows between the regions. The transfer flow $M_{ij}(\cdot)$, $i = 1, 2, \ldots, R$, is controlled such that only a fraction of the flow actually transfers from region i to region j, that is, $u_{ij}(t) \cdot M_{ij}(n_{ij}(t), n_i(t))$, where $0 \leqslant u_{ij}(t) \leqslant 1$. The perimeter control inputs are assumed to be coupled, that is, $u_{ij}(t) + u_{ji}(t) = \epsilon_{ij}$. Such condition is imposed because the perimeter control inputs $u_{ij}(t)$ will be eventually actuated by traffic lights located on the border.

Remark 1

There are different schemes on how to actuate the perimeter control inputs by the traffic lights (e.g., [2, 6]). One simple option would be to equally apply the perimeter control inputs to all traffic lights, where $u_{ij}(t)$ would be the green split from i to j, and $\epsilon_{ij} = 1 - L/C$, $0 < L < C$, where L (sec) is the lost time during cycle C (sec).

3.3. Nonlinear dynamic model with time delay

Note that in (3), as in most of the known MFD-based flow dynamic models that are utilized for control design, it is postulated that vehicles can *immediately* travel from the urban region to its border. However, vehicles are spatially distributed over the whole large region, and their travel times to the border might be *large* that affect the perimeter control process of the traffic dynamics, that is, the perimeter control inputs applied at the current time instant t_c will manipulate the traffic flow composed from traveling vehicles, that reach the border only after a time delay h at time instant $t_c + h$. The travel times needed for vehicles to reach the border should be inherently integrated in the dynamic equations of the system.

Vehicles cannot move immediately from one region to another, as each vehicle needs to travel within the region to approach the perimeter controller at the regional border. Because vehicles are spatially distributed in the region, their travel times to reach the border are different. However, following the aggregated dynamic modeling approach, one can postulate that the average travel time for all vehicles traveling towards the border can be calculated according to the regional MFD. Therefore, the average travel time $h_i(n_i)$ (s) can be considered as an input time delay for the control signal. This time delay can be calculated as follows:

$$h_i(n_i) = \frac{L_i}{V_i} = \frac{n_i}{G_i(n_i)}, \tag{4}$$

where L_i (km) is the average trip length and $V_i = G_i(n_i) \cdot L_i / n_i$ (km/hr) is the average speed. This relation follows from the MFD physical characteristics; refer to [1, 17]. It is important to note that delay $h_i(n_i)$ depends on the number of vehicles in region i; that is, the time delay is *state dependent*.

DOI: 10.1002/rnc

Bearing in mind the presence of time delays in the perimeter control inputs, we rewrite (3) as

$$\begin{aligned}
\dot{n}_{ii}(t) &= -M_{ii}(n_{ii}(t), n_i(t)) + \sum_{j\in S_i} \epsilon_{ij} M_{ji}(n_{ji}(t), n_j(t)) \\
&\quad + \sum_{j\in S_i} \epsilon_{ij} M_{ji}(n_{ji}(t), n_j(t)) u_{ij}(t-h_i) + q_{ii}(t), \\
\dot{n}_{ij}(t) &= -M_{ij}(n_{ij}(t), n_i(t)) u_{ij}(t-h_i) + q_{ij}(t), \\
n_i(t) &= n_{ii}(t) + \sum_{j\in S_i} n_{ij}(t).
\end{aligned} \tag{5}$$

Let us introduce for region i the following state $X_i(t)$, control $U_i(t)$, and disturbance $D_i(t)$ vectors:

$$\begin{aligned}
X_i(t) &= [n_{ii}(t),\ N_i^{\mathrm{T}}(t)]^{\mathrm{T}} \in \mathbb{R}^{\mathrm{card}(S_i)+1}, \quad N_i(t) = \mathbf{Vec}_{j\in S_i} n_{ij}(t) \in \mathbb{R}^{\mathrm{card}(S_i)} \\
U_i(t) &= \mathbf{Vec}_{j\in S_i} u_{ij}(t-h_i) \in \mathbb{R}^{\mathrm{card}(S_i)} \\
D_i(t) &= [q_{ii}(t),\ q_i^{\mathrm{T}}(t)]^{\mathrm{T}} \in \mathbb{R}^{\mathrm{card}(S_i)+1}, \quad q_i(t) = \mathbf{Vec}_{j\in S_i} q_{ij}(t) \in \mathbb{R}^{\mathrm{card}(S_i)}.
\end{aligned} \tag{6}$$

In view of (6), the traffic model (5) can be written as

$$\begin{aligned}
R_i: \quad \dot{X}_i(t) &= \begin{bmatrix} \dot{n}_{ii}(t) \\ \dot{N}_i(t) \end{bmatrix} = -\begin{bmatrix} M_{ii}(n_{ii}(t), n_i(t)) \\ 0 \end{bmatrix} - \begin{bmatrix} b_{oi}^T \\ B_{di} \end{bmatrix} U_i(t) + D_i(t) \\
&\quad + \sum_{j\in S_i} \begin{bmatrix} \epsilon_{ji} M_{ji}(n_{ji}(t), n_j(t)) \\ 0 \end{bmatrix}, \\
n_i(t) &= n_{ii}(t) + \sum_{j\in S_i} n_{ij}(t), \\
Y_i(t) &= n_i(t) = C_i^T X_i(t), \quad C_i^T = \underbrace{[1, \cdots, 1]}_{\mathrm{card}(S_i)+1},\ i = 1, \cdots, R,
\end{aligned} \tag{7}$$

where $Y_i \in \mathbb{R}$, $C_i \in \mathbb{R}^{\mathrm{card}(S_i)+1}$, and

$$\begin{aligned}
b_{oi} &= \mathbf{Vec}_{j\in S_i} M_{ji}(n_{ji}(t), n_j(t)) \in \mathbb{R}^{\mathrm{card}(S_i)}, \\
B_{di} &= \mathbf{Dg}_{j\in S_i} M_{ij}(n_{ij}(t), n_i(t)) \in \mathbb{R}^{\mathrm{card}(S_i)\times \mathrm{card}(S_i)}.
\end{aligned} \tag{8}$$

Now, let us introduce the following block matrices ($i = 1, \cdots, R;\ \ j \in S_i$):

$$\begin{aligned}
-B_i &= \begin{bmatrix} b_{oi}^T \\ B_{di} \end{bmatrix} \in \mathbb{R}^{(1+\mathrm{card}(S_i))\times \mathrm{card}(S_i)}, \\
-F_i\left(n_{ii}(t), n_i(t)\right) &= \begin{bmatrix} M_{ii}(n_{ii}(t), n_i(t))_{1\times 1} \\ 0_{\mathrm{card}(S_i)\times 1} \end{bmatrix} \in \mathbb{R}^{1+\mathrm{card}(S_i)}, \\
F_{ij}\left(n_{ji}(t), n_j(t)\right) &= \begin{bmatrix} \epsilon_{ji} M_{ji}(n_{ji}(t), n_j(t))_{1\times 1} \\ 0_{\mathrm{card}(S_i)\times 1} \end{bmatrix} \in \mathbb{R}^{1+\mathrm{card}(S_j)}.
\end{aligned} \tag{9}$$

Substituting (9) in (7), one obtains the following general nonlinear model for R-region systems with control input delays, operating in the nominal mode (i.e., model that is designed for the nominal MFD):

$$\begin{aligned}
&\dot{X}_i(t) = F_i\left(n_{ii}(t), n_i(t)\right) + B_i\left(n_1(t), \ldots, n_{\mathrm{card}(S_i)}(t)\right) U_i(t) + D_i(t) + \sum_{j\in S_i} F_{ij}\left(n_{ij}(t), n_j(t)\right), \\
&n_i(t) = n_{ii}(t) + \sum_{j\in S_i} n_{ij}(t), \\
&Y_i(t) = n_i(t) = C_i^T X_i(t), \quad C_i^T = \underbrace{[1, \cdots, 1]}_{\mathrm{card}(S_i)+1},\ i = 1, \cdots, R.
\end{aligned} \tag{10}$$

DOI: 10.1002/rnc

4. CONTROL PROBLEM DESCRIPTION

The control problem statement and the adaptive controller design are described in the next sections by focusing on the control problem for one aggregate region, under the dynamic model (10) with $R = 1$. Note that networks with R-region systems can be also considered without altering the methodology in the centralized setting.

4.1. Linearized plant model for one aggregate urban region

Motivated by the model from the previous section, defining new state $x(t)$ and control inputs $u(t)$ as deviations from equilibrium points X_{eq} and U_{eq}, and assuming the time delay $h = h(X_{eq})$, then the linearized system can be derived from (10) in the following canonical (companion) form:

$$\begin{aligned} \dot{x}(t) &= Ax(t) + bu(t-h) + bd(t), \\ y(t) &= Cx(t), \end{aligned} \tag{11}$$

where $x(t) \in \mathbb{R}^2$ and $y(t) \in \mathbb{R}$ are the state and output signals, $d(t) \in \mathbb{R}$ is an equivalent disturbance (i.e., traffic flow demands with destination to the urban region), and $u(t-h) \in \mathbb{R}$ is the delayed control input. The stable matrix $A \in \mathbb{R}^{2\times 2}$ and the vector $b \in \mathbb{R}^{2\times 1}$ are defined by appropriate Jacobian matrices, whose values in the control synthesis are assumed to be unknown.

The linearized system in (11) can be rewritten as an input–output form as follows:

$$y(s) = W(s)e^{-sh}(u(s) + d(s)), \quad W(s) = c^T(sI_n - A)^{-1}b = k_p\frac{N(s)}{D(s)}, \tag{12}$$

where k_p is an unknown constant with a known sign, $D(s) = det(sI_n - A) = s^2 + a_1 s + a_0$, and $N(s) = s + b_0$ are monic stable polynomials with *unknown* constant coefficients. The input time delay $h \in \mathbb{R}^+$ is assumed to be known.

Remark 2
To reflect the plant uncertainty, we assume that the matrices have unknown parameters. That is, it is postulated that the uncertainty in the MFD description is due to varying external conditions; thereat, we view the system model matrices A, b and the coefficients k_p, a_0, a_1, b_0 as unknown elements, and the equivalent external disturbance $d(t)$ as an unknown bounded function with unknown bound d^*.

Remark 3
Note that the set of approximated MFD functions in a given interval (Figure 1) will result after linearization in the same unified model matrices structure, but with different values of its parameters. The use of varying operating points is also incorporated in the linearized dynamics, as different values of the model parameters under the same unified structure.

4.2. Desired control specification

To handle the *plant uncertainties and time delay* for the urban region described by (11)–(12), the control problem is to design adaptive (i) state feedback and (ii) output feedback control laws, and to tune on-line the controller parameters in order to achieve a desired closed-loop specification. The desired specification is to make all signals in the closed-loop system bounded, and the output signal $y(t)$ approximately tracks with small enough error a given reference signal $y_r(t)$ (time varying or constant desired traffic accumulation).

To formalize our control target, we use a reference model that captures the desired system response. The required stable reference model can be expressed as a state-space or an input–output representation. The state-space form is given as follows:

$$\begin{aligned} \dot{x}_r(t) &= A_r x_r(t) + b_r r(t), \\ y_r(t) &= c_r x_r(t), \end{aligned} \tag{13}$$

DOI: 10.1002/rnc

where $A_r \in \mathbb{R}^{2\times 2}$, $b_r \in \mathbb{R}^n$ are known constant matrices, which together with the input signal $r(t) \in \mathbb{R}$ formalize the user-defined reference signal $y_r(t) \in \mathbb{R}$; on the other hand, the input–output form is given as

$$y_r(s) = W_r(s)r(s), \quad W_r(s) = c_r^T(sI_n - A_r)^{-1}b_r = k_r\frac{N_r(s)}{D_r(s)}, \tag{14}$$

where $D_r(s) = det(sI_2 - A_r) = s^2 + a_{r1}s + a_{r0}$ and $N_r(s) = s + b_{r0}$ are monic known stable polynomials and k_r is a known constant.

4.3. Remark on related adaptive control design problems

Before proceeding to design an adaptive control, we briefly digress to review the literature on adaptive tracking and stabilization of systems with input delays. The problem of controlling time-delay systems has been and remains a popular control systems research area, because time delay is a natural component of numerous control applications. The presence of time delays imposes strict limitations on achievable performance and might considerably complicate controller design, because delay elements are infinite dimensional. The latter is an obstacle especially when problems with uncertainties are considered. There are countless published studies on this subject. We refer the reader to, for example, the handbook [11] and the recent monograph [27] for relevant literature.

However, less attention has been given to the topic of tracking adaptive control of plants with input delay, also called dead time. Adaptive control problems for plants with *input delay* are the most difficult in adaptive control theory of delayed plants, mainly because of the plant state prediction over the input delay value under uncertainties. Comparatively few results are available here; we will mention only some substantive early and more recent contributions. In the context of the infinite-dimensional predictor-based feedback laws, a globally stable model reference adaptive control (MRAC) solution for SISO input delayed plants was developed in [28] and later in [29–31]. Recently, within the backstepping framework, a *new approach* (e.g., the books [27, 32]) was developed for the case when the uncertain plant has *unknown* input delays. The input delay is treated as a *transport partial differential equation*, and the dynamic system is represented as a PDE–ODE cascaded system with boundary control.

However, the applicability of these results is limited because all the proposed adaptive control laws are *infinite-dimensional control laws*, that is, utilize finite-time integrals of the delayed control signals, so-called *distributed-delay (DD)* blocks. The impractical DD element is irrational (infinite dimensional), and its precise implementation does not appear to be feasible. Hence, approximations are required (e.g., [11]).

To avoid the problems associated with the approximation, a state feedback Lyapunov-based design was developed in [33] for a class of linear systems with parametric uncertainty and with input and state delays. The design procedure is based on the concept of reference trajectory prediction and does not use DD blocks in the control law. The design MRAC for linear systems with parametric uncertainties and under input delays, based only on the lumped delays, was also studied in the later conference contributions [34, 35]. The design approach in [34, 35] relies on a decomposition of the adaptive control design procedure, where a 'generalized error' in conjunction with two auxiliary linear filters with adjustable gains are introduced. In [34], the problem of sliding-mode state-feedback control for reference state tracking is considered, and in [35], the MRAC problem of output tracking is investigated. The present paper is also in the same spirit of such decomposition procedure, but we introduce upgraded control setups.

5. ADAPTIVE CONTROL DESIGN: THE CASE OF STATE FEEDBACK

5.1. Control setup

We propose a controller structure with two dynamic blocks in series – a non-adaptive Σ_1 and an adaptive Σ_2; see the block diagram in Figure 2. The input signals to the dynamic block labeled Σ_1 are some feedforward $\omega_r(t)$ and feedback $e_G(t)$ signals. The adaptive unit Σ_2 is derived by

DOI: 10.1002/rnc

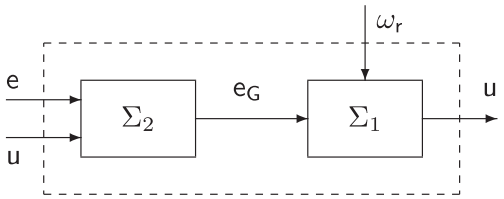

Figure 2. An adaptive controller structure.

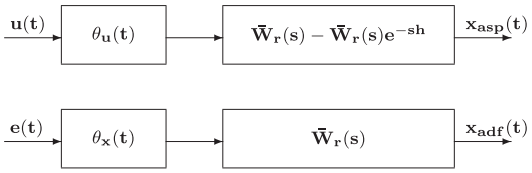

Figure 3. Adaptive Smith predictor and adaptive dynamic filter.

an on-line measured error $e(t)$ and control $u(t)$ signals. The form of $\omega_r(t)$ and $e_G(t)$ will be determined later.

5.1.1. Device Σ_1 description. The non-adaptive controller part Σ_1 is defined as

$$u(t) = -\Gamma_I \omega_r^T(t) \int_0^t \omega_r(t) e_G(t) dt - \Gamma_P \omega_r^T(t) \omega_r(t) e_G(t) - \gamma_I \int_0^t e_G(t) dt \,, \tag{15}$$

where the external reference signal $\omega_r(t) = [r(t)\ x_r(t)]^{\mathrm{T}}$. The matrices $\Gamma_I = \Gamma_I^{\mathrm{T}} > 0$, $\Gamma_P = \Gamma_P^{\mathrm{T}} > 0$, and the scalar $\gamma_I > 0$ are constant design parameters of appropriate dimensions.

5.1.2. Device Σ_2 description. The signal $e_G(t)$, generated by the block Σ_2, comprises two parallel units – an adaptive Smith predictor (ASP) and an adaptive dynamic filter (ADF) – as shown in Figure 3. The proposed ASP is a serial connection of an adjustable gain $\theta_u(t) \in \mathbb{R}$ and the classical Smith predictor, while the ADF is a serial connection of an adjustable gain $\theta_x(t) \in \mathbb{R}^2$ with the reference model. It is important to emphasize that both devices are based on the reference model dynamic rather than the plant dynamic. In both figures, a reference model is represented by its vector transfer function $\bar{W}_r(s)$ from (13) with state-space realizations:

$$\begin{aligned} \text{ASP}: &\quad \dot{x}_{asp}(t) = A_r x_{asp}(t) + b_r \theta_u(t) \Delta_u(t), \quad \Delta_u(t) = [u(t) - u(t-h)] \,, \\ \text{ADF}: &\quad \dot{x}_{adf}(t) = A_r x_{adf}(t) + b_r \theta_x^T(t) e(t) \,. \end{aligned} \tag{16}$$

The output of Σ_2 is a linear transformation with the gain G of the sum of the tracking error $e(t) = x(t) - x_r(t)$, and the internal states $x_{asp}(t) \in \mathbb{R}^n$ and $x_{adf}(t) \in \mathbb{R}^n$, which are the states of ASP and ADF, respectively. As a result, the signal $e_G(t)$ is defined by the following expressions:

$$\begin{aligned} e_G(t) &= G^T e_g(t) \,, \\ e_g(t) &= e(t) + x_{asp}(t) + x_{adf}(t) \,, \\ \dot{\theta}_u(t) &= -\,\mathrm{PI}\big(\gamma_{u1}, \gamma_{u2}, e_G(t)\Delta_u(t)\big) \,, \\ \dot{\theta}_e(t) &= -\,\mathrm{PI}\big(\Gamma_{e1}, \Gamma_{e2}, e_G(t)e(t)\big) \,, \end{aligned} \tag{17}$$

where the symbol $\mathrm{PI}\big(k_I, k_P, z(t)\big)$ denotes the operator

$$\mathrm{PI}\big(k_I, k_P, z(t)\big) = k_I z(t) + k_P \dot{z}(t) \,. \tag{18}$$

DOI: 10.1002/rnc

The gain $G = Pb_r$, and the matrix $P \in \mathbb{R}^{n\times n}$ is a constant matrix such that $P = P^{\mathrm{T}} > 0$ satisfying

$$PA_r + A_r^{\mathrm{T}} P + Q = 0\,, \tag{19}$$

with $Q = Q^T > 0$. The matrices $\Gamma_{e1} = \Gamma_{e1}^{\mathrm{T}} > 0,\ \Gamma_{e2} = \Gamma_{e2}^{\mathrm{T}} > 0$, and the scalars $\gamma_{u1} > 0,\ \gamma_{u2}$ are constant design parameters.

5.2. *Tracking error model and design procedure decomposition*

As it is common in the MRAC theory, we need to express the closed-loop system in terms of the tracking and parameter errors. To design a tracking model, the following lemma is needed; refer to [36].

Lemma 1
There exist some constant vector θ_x^* and scalar θ_r^* that satisfy the plant-model matching equations

$$c^T \left(sI - A - b\theta_x^{*T}\right)^{-1} b\theta_r^* = W_r(s)\,, \qquad (\theta_r^*)^{-1} = k_p k_r^{-1}\,. \tag{20}$$

It is known (see [36]) that pole-zero cancelations are stable for (20); that is, $A + b\theta_x^*$ is a stable matrix. As usually, it is assumed that the sign of θ_r^* is known. Then, after standard manipulations and in view of (20), the tracking error equation for $e_y(t) = y(t) - y_r(t)$ can be written as

$$e_y(t) = W_r(s)\rho^*\big(u(t-h) - \theta_x^{*T} x(t) - \theta_r^* r(t) + \theta_d^* d(t)\big) \tag{21}$$

with $\rho^* = \theta_r^{*-1} = k_p k_r^{-1}$.

Because (20) holds, the reference model may be realized by the triple (A_r, b_r, c_r) and described by the state-space representation (13); refer to [37]. Letting $e(t) = x(t) - x_r(t)$ to be the state error and $e_y(t) = y(t) - y_r(t)$ to be the output error, one obtains the following state-space realization of (21):

$$\begin{aligned} \dot{e}(t) =& A_r e(t) - b\theta_e^{*T} e(t) - b\theta_e^{*T} x_r(t) - b_r r(t) + bd(t) + bu(t-h)\,,\\ e_y(t) =& c^T e(t)\,. \end{aligned} \tag{22}$$

Now, in order to find an error equation parametrization suitable for design, we manipulate (22) by adding and subtracting the terms $bu(t)$, $b_r\theta_u(t)[u(t) - u(t-h)]$, $b_r\theta_e^T(t)e(t)$ with the time-varying vectors $\theta_u(t) \in \mathbb{R}$ and $\theta_e(t) \in \mathbb{R}^2$ from (17). Then, one obtains from (22) the following:

$$\begin{aligned} \dot{e}(t) =& A_r e(t) + b_r\tilde{\theta}_e^T(t)e(t) + b_r\tilde{\theta}_u\Delta_u(t) + bu(t) - b\theta^{*T}\omega_r(t) + bd(t) - b_r\theta_x^T(t)e(t)\\ & - b_r\theta_u(t)\Delta_u(t)\,,\\ e_y(t) =& c^T e(t)\,, \end{aligned} \tag{23}$$

where we introduce, as it is usually carried out in MRAC, the following parameter errors

$$\tilde{\theta}_u(t) = [\theta_u(t) - (\theta_r^*)^{-1}]\,, \quad \tilde{\theta}_e(t) = \theta_e(t) - (\theta_r^*)^{-1}\theta_e^*\,. \tag{24}$$

In (23), the signal $\omega_r(t)$ is from (15) and the unknown vector $\theta^* = [\theta_e^*\ \ \theta_r^*]^T$.

Let us now introduce the auxiliary time-varying scalar $\theta_I(t)$ and vector $\theta(t) \in \mathbb{R}^n$ parameters

$$\begin{aligned} \dot{\theta}_I(t) =& -\gamma_I e_G(t)\,, \quad \theta_I(0) = 0\,,\\ \dot{\theta}(t) =& -\mathrm{PI}\big(\Gamma_I, \Gamma_P, e_G(t)\omega_r(t)\big)\,. \end{aligned} \tag{25}$$

The auxiliary time-varying gains $\theta_I(t)$ and $\theta(t)$ are 'artificial' in the sense that they are used only in the stability proof. Then, using the signal $e_g(t)$ from (17), which is called as a *generalized error*, invoking (15) and (16), and in view of (25), we divide (23) into three coupled equations

DOI: 10.1002/rnc

$$\begin{aligned}\dot{e}_g(t) =& A_r e_g(t) + b_r \tilde{\theta}_e^T(t) e(t) + b_r \tilde{\theta}_u(t) \Delta_u(t) + b \tilde{\theta}^T(t) \omega_r(t) + b d(t) + b \theta_I(t)\,,\\ \dot{x}_{asp} =& A_r x_{asp} + b_r \theta_u(t) \Delta_u(t)\,,\\ \dot{x}_{adf} =& A_r x_{adf} + b_r \theta_x^T(t) e(t)\,,\end{aligned} \tag{26}$$

where $\tilde{\theta}(t) = \theta(t) - \theta^*$. In view of (26), it is clear that the control objective now becomes as follows: the generalized error $e_g(t)$ and the states of ASP and ADF ($x_{asp}(t)$, $x_{adf}(t)$) must be bounded with small enough asymptotic errors.

Inspection of the basic error (26), like in [34, 35], leads to the following observations:

(i) The tracking error equation for $e_g(t)$ has the standard 'classical' so-called bilinear parametric model form, which is generally used for stability analysis and for the design of the adaptation algorithm but for the input delay-free case. Indeed, the input delay is present only as the 'regressor' multiplier $\big(u(t) - u(t-h)\big)$ in the standard adaptive term with the parametric error $\tilde{\theta}_u(t)$ of the adaptive gain $\theta_u(t)$, and the term of this type is removed from the resulting Lyapunov derivative expression, as is usual in conventional MRAC Lyapunov theory.

(ii) Hence, in this way, it is possible *to pull out the input delay from* the design procedure. As a result, we can seek procedures of adaptive control design based on the generalized tracking error equation in the framework of the traditional MRAC technique, with the control objective to stabilize the signal $e_g(t)$ with zero or small enough asymptotic error, and to ensure boundedness of all signals represented in the equation for $e_g(t)$. Indeed, the possibility of such *design decomposition* follows straightforward from the fact that the boundedness of the signal $x_{asp}(t)$ depends only on the boundedness of $\theta_u(t)$ and $u(t)$, as it is evident from (26).

(iii) Therefore, the design process can be decomposed into two consistent phases:

- proof of system signals boundedness and asymptotical convergence of $e_g(t)$ and
- the stability analysis of the resulting closed-loop system.

(iv) To assure the stability of the error model, various modifications of existing adaptive laws can be chosen, based on the available MRAC and robust MRAC techniques.

5.3. Stability results

5.3.1. Lyapunov-like function. To perform steps (ii) and (iii) of the design procedure, that is, to prove the asymptotically convergence of $e_g(t)$, we will use the following Lyapunov-like function

$$\begin{aligned}V =& \sum_{i=1}^{5} V_i\,,\ V_1 = e_g^T(t) P e_g(t)\,,\ V_2 = \tilde{\nu}_e^T(t) \Gamma_{11}^{-1} \tilde{\nu}_e(t)\,,\\ V_3 =& (\theta_r^*)^{-1} \tilde{\nu}_2^T(t) \Gamma_{21}^{-1} \tilde{\nu}_2(t)\,,\ V_4 = \gamma_u^{-1} \tilde{\nu}_u^2(t)\,,\ V_5 = \gamma_I^{-1} (\theta_r^*)^{-1} \tilde{\theta}_I^2(t)\,,\end{aligned} \tag{27}$$

where

$$\begin{aligned}\tilde{\nu}_e(t) =& \tilde{\theta}_e(t) + \Gamma_{12} \nu_e(t)\,, \quad \nu_e(t) = e_G(t) e(t)\,,\\ \tilde{\nu}_2(t) =& \tilde{\theta}(t) + \Gamma_{22} \nu_2(t)\,, \quad \nu_2(t) = e_G(t) \omega_r(t)\,,\\ \tilde{\nu}_u(t) =& \tilde{\theta}_u(t) + \gamma_{u2} \nu_2(t)\,, \quad \nu_u(t) = e_G(t) \Delta_u(t)\,,\\ \tilde{\theta}_I(t) =& \theta_I(t) + \theta_I^* \operatorname{sgn}(e_G(t))\,.\end{aligned} \tag{28}$$

The matrices Q and P are from (19). The parameters $\gamma_I, \gamma_P, \gamma_{u1}, \gamma_{u2}, \Gamma_1$, and Γ_2 are from (15) and (17), and the parameter errors $\tilde{\theta}(t)$, $\tilde{\theta}_u(t)$, and $\tilde{\theta}_I(t)$ are from (24) and (26). The unknown $\theta_I^* \in \mathbb{R}$ will be defined later. The sign function is defined as $\operatorname{sgn}(\star) = 1$, if $(\star) > 0$; $\operatorname{sgn}(\star) = 0$, if $(\star) = 0$; and $\operatorname{sgn}(\star) = -1$, if $(\star) < 0$.

DOI: 10.1002/rnc

5.3.2. The time derivative of the components. In view of (26) and using (19), the time derivative of the components of (27) along the trajectories of the generalized error system (26) is

$$\begin{aligned}\dot{V}_1|_{(26)} =& -e_g^T(t)Q(t)e_g(t) + 2e_G(t)\tilde{\theta}_e^T(t)e(t) + 2e_G(t)\tilde{\theta}_u(t)\Delta_u(t) + 2e_G(t)(\theta_r^*)^{-1}\tilde{\theta}^T(t)\omega_r(t)\\ &+ 2e_G(t)(\theta_r^*)^{-1}d(t) + 2e_G(t)(\theta_r^*)^{-1}\theta_I(t)\,.\end{aligned} \tag{29}$$

Using boundedness of the signal $|d(t)| \leqslant d^*$, one can estimate the term $2e_G(t)\theta_r^{*-1}d(t)$ in (29) as follows:

$$2e_G(t)\theta_r^{*-1}d(t) \leqslant 2|e_G(t)|\left|\theta_r^{*-1}\right|d^*\,. \tag{30}$$

Invoking (15) and (30), (29) yields

$$\begin{aligned}\dot{V}_1|_{(26} =& -e_g^T(t)Q(t)e_g(t) + 2e_G(t)\tilde{\theta}_e^T(t)e(t) + 2e_G(t)\tilde{\theta}_u(t)\Delta_u(t) + 2e_G(t)(\theta_r^*)^{-1}\tilde{\theta}^T(t)\omega_r(t)\\ &+ 2|e_G(t)|\,|\theta_r^*|^{-1}\,\theta_I^* - 2e_G(t)|\theta_r^*|^{-1}\gamma_I\int_0^t e_G(t)dt\,,\end{aligned} \tag{31}$$

where we denote $\theta_I^* = d^*$.

To obtain the time derivative $\dot{V}_2$, we at first note that, in view of (17), the time derivative of $\tilde{\nu}_e(t)$ from (28) is

$$\dot{\tilde{\nu}}_e(t) = \dot{\tilde{\theta}}_e(t) + \Gamma_{12}\dot{\nu}_e(t) = -\Gamma_{12}\nu_e(t)\,. \tag{32}$$

Then, using the last expression and (19), we obtain

$$\dot{V}_2|_{(26)} = -2\tilde{\theta}_e^T(t)e_G(t)e(t) - \nu_e^T(t)\Gamma_{12}\nu_e(t)\,. \tag{33}$$

Following similar calculations, the obtained time derivatives for V_3 and V_4 are

$$\begin{aligned}\dot{V}_3|_{(26)} =& -2\tilde{\theta}^T(t)e_G(t)\omega_r(t) - \nu_2^T(t)\Gamma_{12}\nu_2(t)\,,\\ \dot{V}_4|_{(26)} =& -2\tilde{\theta}_u(t)e_G(t)\Delta_u(t) - \gamma_{u2}\nu_u^2(t)\,.\end{aligned} \tag{34}$$

By using (25), one obtains for $\dot{V}_5$

$$\begin{aligned}\dot{V}_5(t)|_{(26)}^{e_G\neq 0} =& 2\gamma_I^{-1}\,|\theta_r^*|^{-1}\,[\theta_I(t) + \theta_I^*\mathrm{sgn}(e_G(t))]\dot{\theta}_I(t)\\ =& 2e_G(t)|\theta_r^*|^{-1}\gamma_I\int_0^t e_G(t)dt - 2|e_G(t)||\theta_r^*|^{-1}\theta_I^*\\ \dot{V}_5(t)|_{(26)}^{e_G=0} =& 0\,.\end{aligned} \tag{35}$$

Substituting (31)–(35) into (27), we obtain the time derivative for V

$$\dot{V}|_{(26)} = -e_g^T(t)Qe_g(t) \leqslant 0\,, \tag{36}$$

that is, $\dot{V}|_{(26)}$ is (negative) semi-definite. Thus, according to [37], we have proved that $V(t)$ and, therefore, $e_g(t)$, $\tilde{\theta}_e(t)$, $\theta_e(t)$, $\tilde{\theta}(t)$, $\theta(t)$, $\tilde{\theta}_u(t)$, $\theta_u(t)$, $\tilde{\theta}_I(t)$, $\theta_I(t) \in L_\infty$. From (27) and (36), we establish that $e_g(t) \in L_2$. From (26) and closed-loop signal boundedness, we have that $\dot{e}_g(t) \in L_\infty$ so that $e_g(t) \to 0$ as $t \to \infty$.

Further, we show the boundedness of signals $x_{asp}(t)$ and $x_{adf}(t)$. Because $\theta_I(t) \in L_\infty$ and invoking (15) and (25), it follows that $u(t) \in L_\infty$, and then stability of A and boundedness of $d(t)$ guarantee that $x(t) \in L_\infty$. Furthermore, $x_r(t) \in L_\infty$ implies that $e(t) \in L_\infty$, and the definition of the generalized error (26) implies that also $x_{asp}(t), x_{adf}(t) \in L_\infty$. Hence, all signals are bounded.

DOI: 10.1002/rnc

The main result of this section can be summarized as follows.

Theorem 1
Consider the system in (11) and the reference model in (13). Then, invoking Lemma 1, the adaptive control (15)–(17) assures that the closed-loop signals are bounded and that the generalized error $e_g(t)$ converges to zero asymptotically.

6. ADAPTIVE CONTROL DESIGN: THE CASE OF OUTPUT FEEDBACK

In this section, we develop a direct *output* feedback adaptive scheme for the uncertain linearized model (12) to ensure the control objective (14), despite the plant parameters and disturbance (demand) uncertainties and input delay presence. We represent the design steps and mainly focus on the basic error system model formulation, which will lead us to another control structure.

6.1. Basic tracking error model design

Step 1. In view of the conventional assumptions [36, 37] on the reference model (14) and the part of plant without input time delay $W(s)$ (12), it is possible to write the following *actual error model* for $e_y(t) = y(t) - y_r(t)$ instead of (22):

$$e_y = W_r(s)\rho^*\Big[u(t-h) - \theta_y^* y(t) - \theta_1^* x_1(t) - \theta_2^* x_2(t) - \theta_r^* r(t) + \big(1 - \theta_1^{*T} W_f(s)\big)d(t)\Big], \tag{37}$$

where

$$x_1 = W_f(s)[u]\,,\ x_2 = W_f(s)[y]\,,\ W_f(s) = \frac{1}{s+\lambda_0},\ \lambda_0 > 0.$$

$\theta_1^*, \theta_2^*, \theta_y^*, \theta_r^* \in \mathbb{R}$ are the so-called matching parameters.

Step 2. Next, we add and subtract to right side of (37) the terms $W_r(s)\rho^*\big[u(t)\big]$ and $W_r(s)\big[\theta_u(t)\Delta_u(t)\big]$ with the adjustable gain $\theta_u(t) \in \mathbb{R}$. Then, one obtains from (37) the following:

$$\begin{aligned} e_y =& W_r(s)\rho^*\Big[u(t) - \theta_y^* y(t) - \theta_1^* x_1(t) - \theta_2^* x_2(t) - \theta_r^* r(t) + \big(1 - \theta_1^{*T} W_f(s)\big)d(t)\Big] \\ &+ W_r(s)\big[\tilde{\theta}_u(t)\Delta_u(t)\big] - W_r(s)\big[\theta_u(t)\Delta_u(t)\big] \end{aligned} \tag{38}$$

where as in (24), $\tilde{\theta}_u(t)$ is the parameter error.

Step 3. Further, we introduce the new signal $y_{asp}(t)$, which is generated as

$$y_{asp}(t) = W_r(s)\left(\theta_u(t)\Delta_u(t)\right)\ . \tag{39}$$

That is, we replaced the two blocks ASP and ADF from (16) (Figure 3) by one block.

Step 4. In contrast to (17) from Section 5, now it is proposed to define the generalized error in the form $e_{gy}(t) = e_y(t) + y_{asp}(t)$ and to determine the control law as

$$u(t) = \Theta^T(t)\Omega(t) - \gamma_I \int_0^t e_{gy}(t)dt \tag{40}$$

where $\Theta(t)$ is the on-line updated vector gain, $\Omega(t) = [e_{gy}(t)\ \ x_1(t)\ \ x_2(t)\ \ y_r(t)\ \ r(t)\ \ y_{asp}(t)]^T$ is the regressor vector, and $\gamma_I > 0$ is a design parameter.

Step 5. Finally, similarly with (26) from Section 5 after decomposition, we obtain the basic error model for the adaptive control algorithms design and stability analysis

DOI: 10.1002/rnc

Table I. Adaptive output feedback controller.

Control law	$u(t) = \Theta^T(t)\Omega(t) - \gamma_I \int_0^t e_{gy}(t)dt$
Regressor vector	$\Omega(t) = [e_{gy}(t)\ x_1(t)\ x_2(t)\ y_r(t)\ r(t)\ y_{asp}(t)]^T$
Filters	$x_1(t) = W_f(s)[u],\ x_2(t) = W_f(s)[y]$
Control gain update law	$\dot{\Theta}(t) = -\mathrm{PI}\left(\Gamma_I, \Gamma_P, e_{gy}(t)\Omega(t)\right)$
Generalized error	$e_{gy}(t) = e_y(t) + y_{asp}(t) = y(t) - y_r(t) + y_{asp}(t)$
Adaptive Smith compensator	$y_{asp}(t) = W_r(s)\left(\theta_u(t)\Delta_u(t)\right)$
Adaptive compensator gain update law	$\dot{\theta}_u(t) = -\mathrm{PI}\left(\gamma_{u1}, \gamma_{u1}, e_{gy}(t)\Delta_u(t)\right)$

$$
\begin{aligned}
e_{gy} =& W_r(s)\rho^*\left(\tilde{\Theta}^T(t)\Omega(t)\right) + W_r(s)\left(\tilde{\theta}_u(t)\Delta_u(t)\right) - \gamma_I \int_0^t e_{gy}(t)dt \\
&+ W_r(s)\rho^*\left(1 - \theta_1^{*T} W_f(s)\right)d(t)\,, \\
y_{asp} =& W_r(s)\left(\theta_u(t)\Delta_u(t)\right)
\end{aligned}
\tag{41}
$$

where $\tilde{\Theta}(t)$ is the usual parameter error vector.

Then, the following theorem sets the adaptive controller, which provides the desired closed-loop specification defined in Subsection 4.2.

Theorem 2
Consider the plant defined in (12) and the reference model (14). Then, the boundedness of the closed-loop signals and convergence of the generalized error $e_{gy}(t)$ to zero asymptotically can be assured by the adaptive controller in Table I, where the matrices $\Gamma_I = \Gamma_I^T > 0$, $\Gamma_P = \Gamma_P^T > 0$, $\Gamma_1 = \Gamma_1^T > 0$, $\Gamma_2 = \Gamma_2^T > 0$ and the scalars $\gamma_I > 0$, $\gamma_{u1} > 0$, and $\gamma_{u2} > 0$ are the constant design parameters of appropriate dimensions and the symbol $\mathrm{PI}(z(t))$ is from (18).

Proof
The proof is presented in the Appendix. □

7. SIMULATION CASE STUDY FOR AN URBAN REGION

7.1. The model under consideration

The underling linearized regional dynamic model is based on the MFD parametrization, whose pattern matches the MFD observed in Yokohama [17]. We denote all the signals corresponding to this underling MFD's model (prototype) by the index 'yok'. To reflect the interval MFD shape, two types of potential parametric model uncertainties are studied: (i) variation in the MFD shape, because the flow of the urban region is subjected to different perturbations, for example, hysteresis phenomena have been found to exist [12–15], and (ii) possible uncertainties as a result of using various operation points for model linearization. That is, for the item (i), we allow deviations of the prototype model shape (after normalization) by ±40%, that is, the uncertain plant transfer function $W(s) \in [W_{0.6yok}(s)\ \ W_{1.4yok}(s)]$, where $W_{0.6yok}(s)$ and $W_{1.4yok}(s)$ respectively match $0.6MFD_{yok}$ and $1.4MFD_{yok}$, and $W_{yok}(s)$ corresponds to the MFD observed in Yokohama. While for the item (ii), in order to cover various possible working conditions, we have investigated the following operation points $n_{eq} = 0.8n_{cr}$, $n_{eq} = 0.9n_{cr}$, and $n_{eq} = 0.95n_{cr}$. The critical accumulation n_{cr} corresponds to an optimum regional accumulation at which a maximum flow is reached for different uncertainties. For the nominal MFD fitting approximation, we use a third-order polynomial function normalized by the maximum value of accumulation $n_{\max}$.

The transfer functions of the linearized system around the various operation points, $n_{eq} = 0.8n_{cr}$, $n_{eq} = 0.9n_{cr}$, and $n_{eq} = 0.95n_{cr}$, for the different MFD pattern approximations are presented in Table II.

The step responses of the dynamical region model for all considered cases with a particular value of delay $h = 10$ are depicted in Figure 4, while the step responses for different values of time delay $h = h(n_{eq})$ are shown in Figure 5, where the time-delay value depends on the chosen operation

DOI: 10.1002/rnc

Table II. Transfer functions utilized in the simulation study.

	$n_{eq} = 0.8n_{cr}$	$n_{eq} = 0.9n_{cr}$	$n_{eq} = 0.95n_{cr}$
$W_{yok}(s)$	$1.972\frac{s+14.59}{(s+1.865)(s+15.43)}$	$0.9014\frac{s+13.2}{(s+0.9064)(s+13.13)}$	$0.4352\frac{s+12.56}{(s+0.4523)(s+12.09)}$
$W_{0.6yok}(s)$	$2.295\frac{s+10.39}{(s+2.286)(s+10.43)}$	$1.0665\frac{s+9.377}{(s+1.086)(s+9.205)}$	$0.5170\frac{s+8.915}{(s+0.5326)(s+8.655)}$
$W_{1.4yok}(s)$	$1.326\frac{s+18.79}{(s+1.206)(s+20.66)}$	$0.5865\frac{s+17.03}{(s+0.5807)(s+17.2)}$	$0.2809\frac{s+16.2}{(s+0.2918)(s+15.6)}$

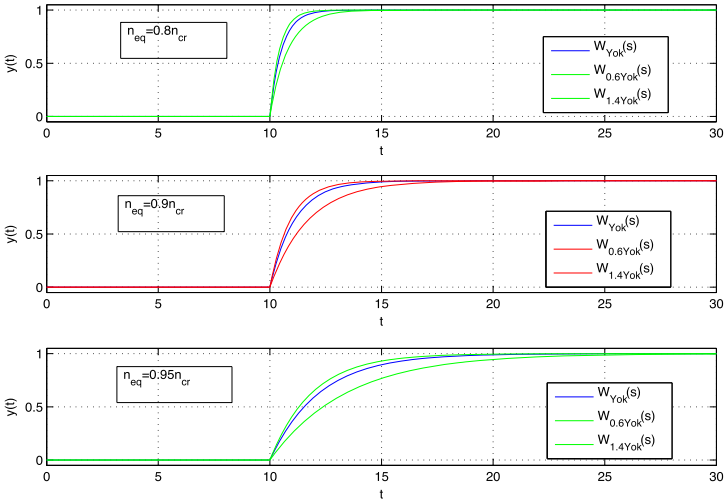

Figure 4. The step responses corresponding to normalized system transfer functions for various cases of the macroscopic fundamental diagram parametrization and for three different linearization operation points $n_{cr} = 0.8,\ 0.9,\ 0.95$.

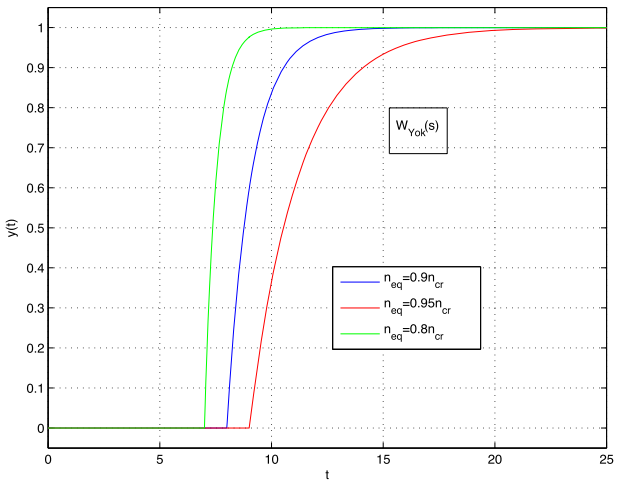

Figure 5. The step responses for the normalized system transfer function $W_{yok}(s)$, under three different linearization operation points: $n_{eq} = 0.8n_{cr}$, $n_{eq} = 0.9n_{cr}$, and $n_{eq} = 0.95n_{cr}$.

point of the linearization n_{eq} and is calculated according to (4). The presented step responses in Figure 5 are for the prototype-model $W_{yok}(s)$.

7.2. The simulation results of adaptive control designs

In this simulation study, we apply the adaptive controller from Table I to different plant models with transfer functions from Table II. The design parameter values of the controller are chosen as

DOI: 10.1002/rnc

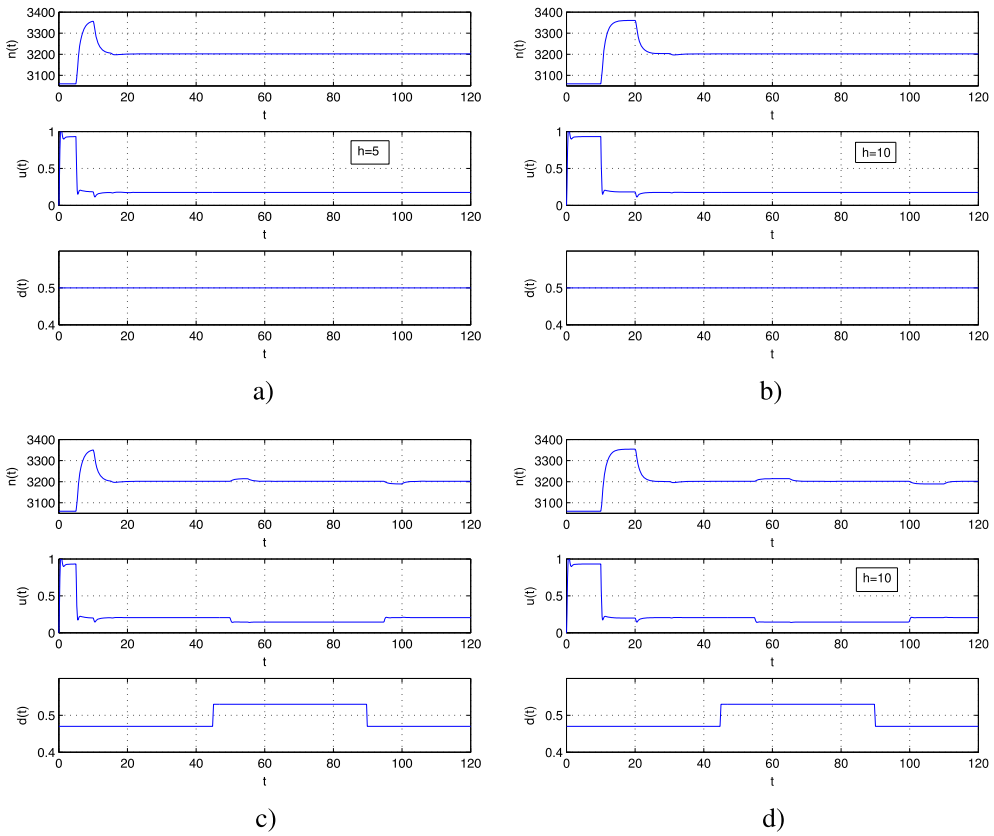

Figure 6. Simulation results for the adaptive output feedback controller from Table I with $n_{eq} = 0.9n_{cr}$. The graphs show the time history of the regional accumulation $n(t)$, the control input $u(t)$, and the demand $d(t)$ for two different time delays – $h = 5$ in (a) and (c), and $h = 10$ in (b) and (d) – and for two different demands – unknown constant demand in (a) and (b), and unknown time-varying demand in (c) and (d).

$\Gamma_I = 9I_{2\times2}$, $\Gamma_P = 2I_{2\times2}$, $\gamma_I = 9$, $\gamma_{u2} = 2$, $\gamma_{u1} = 9$, $\Gamma_1 = 9I_{2\times2}$, and $\Gamma_2 = 2I_{2\times2}$, while the reference model is chosen as $W_r(s) = k_r \frac{1}{s+a_r}, k_r = 1.5, a_r = 1$.

Remark 4

Note that the plant parameter values and the value of the disturbance d are assumed to be unknown for the controller. Furthermore, the reference model and the controller's design parameter values, that is, Γ_I, Γ_P, γ_I, γ_{u2}, γ_{u1}, Γ_1, and Γ_2, are the same for all investigated cases.

The equivalent bounded disturbance d, that is, the exogenous traffic flow demand with destination to the urban region, is chosen in the different experiments as (i) an unknown constant or (ii) as an unknown function of time (unknown time-varying demand). Simulation results for the adaptive output feedback controller from Table I are presented in Figure 6 for $n_{eq} = 0.9n_{cr}$, while in Figure 7, the results are presented for $n_{eq} = 0.95n_{cr}$. The graphs show the time history of the regional accumulation $n(t)$, the control input $u(t)$, and the demand $d(t)$ for two different time delays – $h = 5$ in (a) and (c), and $h = 10$ in (b) and (d) – and for two different demands – unknown constant demand in (a) and (b), and unknown time-varying demand in (c) and (d).

As verified by simulation results, the desired system performance is achieved: all the closed-loop signals are bounded, the plant output converges to a predetermined value as expected according to Theorem 2. Figures 6 and 7 show that the transient performance changes slightly for (i) different values of plant transfer functions from Table II; (ii) various values of input time delays; and (iii) both constant and time-varying demand signals under the same controller parameters, initial conditions, and model reference inputs.

DOI: 10.1002/rnc

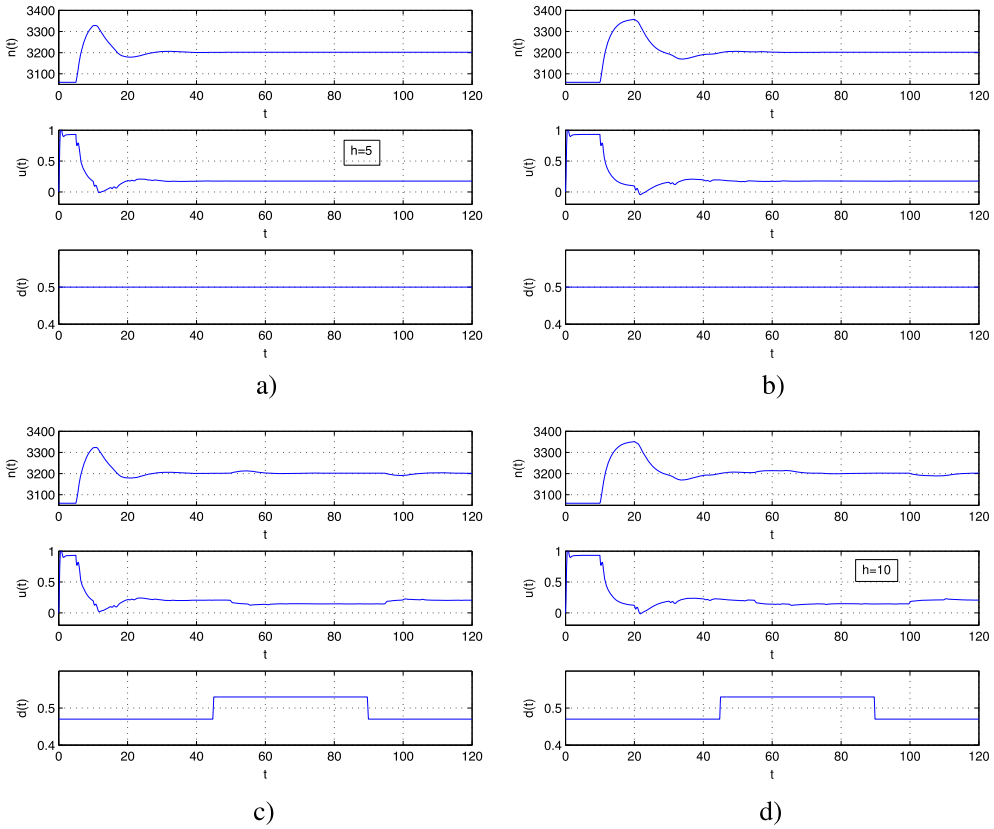

Figure 7. Simulation results for the adaptive output feedback controller from Table I with $n_{eq} = 0.95n_{cr}$. The graphs show the time history of the regional accumulation $n(t)$, the control input $u(t)$, and the demand $d(t)$ for two different time delays – $h = 5$ in (a) and (c), and $h = 10$ in (b) and (d) – and for two different demands – unknown constant demand in (a) and (b), and unknown time-varying demand in (c) and (d).

Remark 5

The adaptive controller was simulated only for a simplified mathematical plant representation – linearized model with parameter and external perturbations. Before implementing the adaptive controller in reality, it is required to further test it on more sophisticated system models taking into account nonlinearities, possible failures, and so on.

8. CONCLUDING REMARKS

In this paper, we have developed a more realistic MFD-based nonlinear control-oriented model for urban traffic networks with time delays incorporated into model structure. Based on the concept of interval MFD for robust modeling, and considering the linearized model with unknown coefficients subject to an input time delay and unknown bounded disturbance, we have developed two new perimeter control schemes for one aggregated urban traffic region under unknown bounded external disturbances and parameter uncertainties. The proposed approach for designing feedback control strategies is performed in the context of MRAC theory and leads to tractable design formulations for *state feedback*, when the plant state is measured, that is, the number of vehicles from all regional origins to regional destinations are measured, and *output feedback*, when the system output is only measured, that is, only the total number of vehicles in all regions are measured. The key feature of the developed design procedure is that it converts the adaptive control design problem with input delay into two separate problems – a delay-free conventional MRAC problem and the Smith predictor (based on reference rather than plant model) with adjustable gain problem.

DOI: 10.1002/rnc

Although in this paper the MRAC approach has only been stated in the context of a simplified model for one aggregated urban region (the state $x(t) \in \mathbb{R}^2$), we believe that it is applicable for the case of a multi-region system, where the states and the control inputs are vectors. In addition, we believe that because the form of h does not change the basic error equations structure, the proposed design procedure is applicable also for various MRAC problems with non-constant input delays. These issues are currently under investigation.

APPENDIX: PROOF OF THEOREM 2

A typical procedure of MRAC is used to study the closed-loop stability (e.g., [37]). The augmented vector $\hat{x}(t) = [x \ x_1 \ x_2]^T$ is introduced, and the state of the corresponding non-minimal realization $\hat{c}^T(sI - \hat{A})^{-1}\hat{b}\theta_r^*$ of W_r is denoted by $\hat{x}_r(t)$. Then, one can write the following state-space representation for (41)

$$\begin{aligned}\frac{d\hat{e}(t)}{dt} =& \hat{A}\hat{e}(t) + \bar{b}\rho^*\left\{\tilde{\Theta}^T(t)\Omega(t) + \tilde{\theta}_u(t)\Delta_u(t) + \left(1 - \theta_1^{*T}H(s)\right)[d(t)] - \gamma_I\int_0^t e_{gy}(t)dt\right\} \\ e_{gy}(t) =& \hat{c}^T\hat{e}(t),\end{aligned} \tag{42}$$

where $\bar{b} = \hat{b}\theta_r^*$ and $\rho^* > 0$. Because $\hat{c}^T(sI - \hat{A})^{-1}\hat{b}\theta_r^* = W_r$ is strictly positive real, there exists a matrix $\hat{P} = \hat{P}^T > 0$ satisfying

$$\hat{A}^T\hat{P} + \hat{P}\hat{A} + \nu\xi^T + \hat{Q} = 0, \quad \hat{P}\hat{b}\theta_r^* = \hat{c}, \tag{43}$$

where ν is a vector and $\hat{Q} = \hat{Q}^T > 0$ is any positive-definite matrix [37, pp.129–130].

Now, similarly as in (27), we introduce the following Lyapunov-like function:

$$\hat{V} = \sum_{i=1}^{4} V_i\,,\ V_1 = \hat{e}^T(t)\hat{P}\hat{e}(t)\,,\ V_2 = \tilde{\nu}^T(t)\Gamma_{11}^{-1}\tilde{\nu}(t)\,,\ V_3 = \gamma_u^{-1}\tilde{\nu}_u^2(t)\,,\ V_4 = \gamma_I^{-1}\rho^*\tilde{\theta}_I^2(t)\,, \tag{44}$$

where

$$\begin{aligned}\tilde{\nu}(t) =& \tilde{\theta}(t) + \Gamma_{12}\nu(t)\,, \quad \nu(t) = e_{gy}(t)\Omega(t)\,, \\ \tilde{\nu}_u(t) =& \tilde{\theta}_u(t) + \gamma_{u2}\nu_2(t)\,, \quad \nu_u(t) = e_{gy}(t)\Delta_u(t)\,, \\ \tilde{\theta}_I(t) =& \theta_I(t) + \theta_I^*\mathrm{sgn}(e_{gy}(t))\,.\end{aligned} \tag{45}$$

The 'virtual' scalar adaptation gain $\theta_I(t)$ and the positive constant θ_I^* will be defined later. The matrices $\hat{Q}$ and $\hat{P}$ are from (43) and the remaining notations are identical to (27) and (28).

Using (43), the time derivative $\dot{V}_1(t)$ of (44) along with (42) can be written as

$$\begin{aligned}\dot{V}_1(t)|_{(42)} =& -\hat{e}^T(t)Q\hat{e}(t) - \hat{e}^T(t)\nu\xi^T\hat{e}(t) + 2\rho^*\hat{e}^T(t)P\bar{b}\tilde{\Theta}^T(t)\Omega(t) + 2\rho^*\hat{e}^T(t)P\bar{b}\tilde{\theta}_u(t)\Delta_u(t) \\ & - 2\hat{e}^T(t)P\bar{b}\rho^*\gamma_I\int_0^t e_{gy}(t)dt + 2\hat{e}^T(t)P\bar{b}\rho^*\left(1 - \theta_1^{*T}H(s)\right)[d(t)]\,.\end{aligned} \tag{46}$$

In view of boundedness of $d(t)$, we can estimate the last term of (46) as

$$2\hat{e}^T(t)P\bar{b}\rho^*\left(1 - \theta_1^{*T}H(s)\right)[d(t)] \leqslant 2|e_{gy}(t)||\rho^*|\left|\left|\left(1 - \theta_1^{*T}H(s)\right)\right|\right|_\infty |d(t)| = 2\nu^*\rho^*|e_{gy}(t)| \tag{47}$$

where $\nu^* = \left|\left|\left(1 - \theta_1^{*T}H(s)\right)\right|\right|_\infty d^*$. Here, we used the fact that $\hat{c}^T\hat{e}(t) = e_{gy}(t)$; see (42) and (43). Invoking (47) and (46), one obtains

DOI: 10.1002/rnc

$$\dot{V}_1(t)|_{(42)} \leqslant -\hat{e}^T(t)Q\hat{e}(t) - \hat{e}^T(t)\nu\xi^T\hat{e}(t) + 2\rho^*\hat{e}^T(t)P\bar{b}\tilde{\Theta}^T(t)\Omega(t) + 2\rho^*\hat{e}^T(t)P\bar{b}\tilde{\theta}_u(t)\Delta_u(t) - 2\rho^*\gamma_I e_{gy}(t)\int_0^t e_{gy}(t)dt + 2\eta^*\rho^*|e_{gy}(t)|\,. \tag{48}$$

Similarly as in (32)–(34), we obtain the time derivatives $\dot{V}_2(t)$ and $\dot{V}_3(t)$ as follows:

$$\begin{aligned}\dot{V}_2|_{(42)} &= -2\tilde{\Theta}^T(t)\Omega(t)e_{gy}(t) - \nu^T(t)\Gamma_{12}\nu(t)\,,\\ \dot{V}_3|_{(42)} &= -2\tilde{\theta}_u(t)e_{gy}(t)\Delta_u(t) - \gamma_{u2}\nu_u^2(t)\,.\end{aligned} \tag{49}$$

Let us now define $\theta_I^* = \nu^*$ and the 'virtual' adaptation gain $\theta_I(t)$ in (45) as

$$\dot{\theta}_I(t) = -\gamma_I e_{gy}(t)\,, \quad \theta_I(0) = 0\,. \tag{50}$$

Then in view of (50), we obtain for $\dot{V}_4(t)$

$$\begin{aligned}\dot{V}_4(t)|_{(41)}^{e_{gy}\neq 0} &= 2\gamma_I^{-1}\rho^*[\theta_I(t) + \theta_I^*\mathrm{sgn}(e_{gy}(t))]\dot{\theta}_I(t)\\ &= 2\rho^*\gamma_I e_{gy}(t)\int_0^t e_{gy}(t)dt - 2\nu^*\rho^*|e_{gy}(t)|\\ \dot{V}_4(t)|_{(41)}^{e_{gy}=0} &= 0\,.\end{aligned} \tag{51}$$

Applying (48), (49), and (51) to (44), we obtain the time derivative for V

$$\dot{V}|_{(42)} = -\hat{e}^T(t)Q\hat{e}(t) - \hat{e}^T(t)\nu\xi^T\hat{e}(t) \leqslant 0\,, \tag{52}$$

that is, $\dot{V}|_{(42}$ is (negative) semi-definite. This fact is central to the remainder of the stability analysis, which follows directly using similar steps as in a previous section.

ACKNOWLEDGEMENT

This work was supported by the European Union's Seventh Framework Programme grant no. (FP7/2007-2013)630690 - MC–SMART.

REFERENCES

1. Daganzo CF. Urban gridlock: macroscopic modeling and mitigation approaches. *Transportation Research Part B* 2007; **41**(1):49–62.
2. Keyvan-Ekbatani M, Kouvelas A, Papamichail I, Papageorgiou M. Exploiting the fundamental diagram of urban networks for feedback-based gating. *Transportation Research Part B* 2012; **46**(10):1393–1403.
3. Haddad J, Shraiber A. Robust perimeter control design for an urban region. *Transportation Research Part B* 2014; **68**:315–332.
4. Haddad J, Geroliminis N. On the stability of traffic perimeter control in two-region urban cities. *Transportation Research Part B* 2012; **46**(1):1159–1176.
5. Geroliminis N, Haddad J, Ramezani M. Optimal perimeter control for two urban regions with macroscopic fundamental diagrams: a model predictive approach. *IEEE Transactions on Intelligent Transportation Systems* 2013; **14**(1):348–359.
6. Aboudolas K, Geroliminis N. Perimeter and boundary flow control in multi-reservoir heterogeneous networks. *Transportation Research Part B* 2013; **55**:265–281.
7. Hajiahmadi M, Haddad J, Schutter BD, Geroliminis N. Optimal hybrid perimeter and switching plans control for urban traffic networks. *IEEE Transactions on Control Systems Technology* 2015; **23**:464–478.
8. Haddad J, Ramezani M, Geroliminis N. Cooperative traffic control of a mixed network with two urban regions and a freeway. *Transportation Research Part B* 2013; **54**:17–36.
9. Hajiahmadi M, Haddad J, Schutter B D, Geroliminis N. Optimal hybrid macroscopic traffic control for urban regions: perimeter and switching signal plans controllers. *European Control Conference 13*, Zürich, 17–19 July 2013; 3500–3505.
10. Keyvan-Ekbatani M, Papageorgiou M, Papamichail I. Perimeter traffic control via remote feedback gating. *16th EURO Working Group on Transportation Meeting*, Published in Procedia - Social and Behavioral Sciences 111 (2014), Porto, Portugal, 2013; 645–653.

DOI: 10.1002/rnc

11. Mirkin L, Palmor ZJ. Control issues in systems with loop delays. In *Handbook of Networked and Embedded Control Systems*, Hristu-Varsakelis D, Levine WS (eds). Birkhäuser: Basel, 2005; 627–648.
12. Daganzo CF, Gayah VV, Gonzales EJ. Macroscopic relations of urban traffic variables: bifurcations, multivaluedness and instability. *Transportation Research Part B* 2011; **45**(1):278–288.
13. Buisson C, Ladier C. Exploring the impact of homogeneity of traffic measurements on the existence of macroscopic fundamental diagrams. *Transportation Research Record* 2124; **2009**:127–136.
14. Saberi M, Mahmassani H. *Exploring Properties of Network-wide Flow-Density Relations in a Freeway Network*. Transportation Research Board 91st Annual Meeting: Washington, D.C., 2012.
15. Geroliminis N, Sun J. Hysteresis phenomena of a macroscopic fundamental diagram in freeway networks. *Transportation Research Part A* 2011; **45**(9):966–979.
16. Godfrey JW. The mechanism of a road network. *Traffic Engineering and Control* 1969; **11**(7):323–327.
17. Geroliminis N, Daganzo CF. Existence of urban-scale macroscopic fundamental diagrams: some experimental findings. *Transportation Research Part B* 2008; **42**(9):759–770.
18. Ji Y, Daamen W, Hoogendoorn S, Hoogendoorn-Lanser S, Qian X. Macroscopic fundamental diagram: investigating its shape using simulation data. *Transportation Research Record* 2161; **2010**:42–48.
19. Mazloumian A, Geroliminis N, Helbing D. The spatial variability of vehicle densities as determinant of urban network capacity. *Philosophical Transactions of the Royal Society A: Mathematical, Physical and Engineering Sciences* 2010; **368**(1928):4627–4647.
20. Gayah VV, Daganzo CF. Clockwise hysteresis loops in the macroscopic fundamental diagram: an effect of network instability. *Transportation Research Part B* 2011; **45**(4):643–655.
21. Zhang L, Garoni T, de Gier J. A comparative study of macroscopic fundamental diagrams of arterial road networks governed by adaptive traffic signal systems. *Transportation Research Part B* 2013; **49**:1–23.
22. Mahmassani H, Williams J, Herman R. Performance of urban traffic networks. *Proceedings of the 10th International Symposium on Transportation and Traffic Theory* Gartner N, Wilson N (eds)., Elsevier, Amsterdam, The Netherlands, 1987.
23. Olszewski P, Fan HSL, Tan YW. Area-wide traffic speed-flow model for the Singapore CBD. *Transportation Research Part A* 1995; **29A**(4):273–281.
24. Geroliminis N, Sun J. Properties of a well-defined macroscopic fundamental diagram for urban traffic. *Transportation Research Part B* 2011; **45**(3):605–617.
25. Knoop V, Hoogendoorn S, van Lint H. The impact of traffic dynamics on the macroscopic fundamental diagram. *92nd Annual Meeting of Transportation Research Board*, Washington D.C., USA, 2013.
26. Mahmassani HS, Saberi M, Zockaie AK. Network gridlock: theory, characteristics, and dynamic. *Procedia - Social and Behavioral Sciences* 2013; **80**:79–98. DOI: 10.1016/j.sbspro.2013.05.007, 20th International Symposium on Transportation and Traffic Theory.
27. Krstić M. *Delay Compensation for Nonlinear, Adaptive, and PDE Systems*. Birkhauser: Boston, 2009.
28. Ortega R, Lozano R. Globally stable adaptive controller for systems with delay. *International Journal of Control* 1988; **47**(1):17–23.
29. Niculescu SI, Annaswamy AM. An adaptive smith-controller for time-delay systems with relative degree $n^* \leqslant 2$. *System Control Letters* 2003; **49**(5):347–358.
30. Yildiz Y, Annaswamy A, Kolmanovsky I, Yanakiev D. Adaptive posicast controller for time-delay systems with relative degree $n^* \leqslant 2$. *Automatica* 2010; **46**:279–289.
31. Dydek Z, Annaswamy A, Slotine J, Lavretsky E. High performance adaptive control in the presence of time delays. *Proceedings of the American Control Conference*, Marriott Waterfront, Baltimore, MD, USA, 2010; 880–885.
32. Bekiaris-Liberis N, Krstić M. *Nonlinear Control Under Nonconstant Delays*. SIAM: Philadelphia, 2013.
33. Mirkin BM, Mirkin EL, Gutman PO. State-feedback adaptive tracking of linear systems with input and state delays. *International Journal of Adaptive Control and Signal Processing* 2009; **23**(6):567–580.
34. Mirkin B, Gutman PO, Shtessel Y. Adaptive control with asymptotical sliding mode of uncertain plants with input and state delay. *13th International Workshop on Variable Structure Systems*, Nantes, France, 2014; 132–136. June 29 to July 2nd.
35. Mirkin B, Gutman PO, Shtessel Y. A new output feedback adaptive input time-delay compensation scheme for uncertain systems. *19th International Conference on Methods and Models in Automation and Robotics*, 177–182, 2–5 September 2014.
36. Tao G. *Adaptive Control Design and Analysis*. John Wiley and Sons: New York, 2003.
37. Ioannou PA, Sun J. *Robust Adaptive Control*. Prentice-Hall: New Jersey, 1996.

DOI: 10.1002/rnc